On Gaussian Curvature and Membrane Fission

Mara Denisse Rueda-Contreras
Institute of Physics, UNAM
Andreu F. Gallen
University of Barcelona
J. Roberto Romero-Arias (romero@mym.iimas.unam.mx)
Institute for Research in Applied Mathematics and Systems, UNAM
Aurora Hernandez-Machado
Institut Català de Nanociència i Nanotecnologia
Rafael A. Barrio
Institute of Physics, UNAM

Research Article

Keywords: Gaussian, fission, modulus, evolution

Posted Date: February 4th, 2021

DOI: https://doi.org/10.21203/rs.3.rs-156372/v1

On Gaussian curvature and membrane fission

Mara Denisse Rueda-Contreras[1], Andreu F. Gallen[2], J. Roberto Romero-Arias[3,*], Aurora Hernandez-Machado[2,4], and Rafael A. Barrio[1]

[1]nstituto de Física, U.N.A.M., 01000, Ap. Postal 101000, México D.F., México
[2]Departament Física de la Matèria Condensada, Universitat de Barcelona, E-08028 Barcelona, Spain
[3]Instituto de Investigaciones en Matemáticas Aplicadas y en Sistemas, Universidad Nacional Autónoma de México, 01000 Ciudad de México, Mexico
[4]Institute of Nanoscience and Nanotechnology (IN2UB), 08028 Barcelona, Spain
[*]romero@mym.iimas.unam.mx

ABSTRACT

We propose a three-dimensional mathematical model to describe dynamical processes of membrane fission. The model is based on a phase field equation that includes the Gaussian curvature contribution to the bending energy. With the addition of the Gaussian curvature energy term numerical simulations agree with the predictions that tubular shapes can break down into multiple vesicles. A dispersion relation obtained with linear analysis predicts the wavelength of the instability and the number of formed vesicles. Finally, a membrane shape diagram is obtained for the different Gaussian and bending modulus, showing different shape regimes.

Introduction

Vesicle formation is a fundamental process in many biological systems, e.g., the Golgi apparatus[1,2], the synaptic system[3,4], or enveloped viruses[5,6]. The Golgi apparatus constantly releases transport vesicles filled with proteins that are carried to other parts of the cell. In the synaptic nerve terminals, vesicles are filled with neurotransmitters and released by exocytosis[3]. Moreover, many viruses are enveloped by a lipid membrane which mediates the fusion of the virus with the host cell membrane; some examples are HIV-1, herpesviruses, the Ebola virus[5], and coronaviruses[7] like SARS-CoV-2.

There is a fair amount of research on cellular membrane deformation and morphology[8,9]. However, there is little understanding when topological transitions occur and Gaussian curvature plays a role[8–10]. The Gauss-Bonnet theorem states that the integral of the Gaussian curvature over a surface is proportional to the surface Euler characteristic[11]. This assures that the Gaussian curvature term is topologically invariant. This leads to the term being ignored for homogeneous systems. However, it is fundamental for topological transitions like fusion or fission. Lipid bilayers exhibit different stable configurations, depending on the values of the Gaussian and bending energetic moduli. There are no direct experimental measurements of the Gaussian modulus, although a method has been proposed recently[12]. Indirect measurements give a negative value of about $\bar{\kappa}' \approx -15 K_B T$[13], and molecular dynamics simulations give similar results[14]. The negative sign implies that the energetic term of the Gaussian curvature favors fission, since fission increases the Euler characteristic. The most common fission event is the formation of a vesicle.

In all cases what seems a necessary requirement for fission is a large membrane curvature on the area where a vesicle is to be generated, which can be modeled with a spontaneous curvature. The final fission of the vesicle is often mediated by very specific proteins, although this is not always the case. Large spontaneous curvature can suffice to produce fission[15–17]. This can be accomplished by interactions among membrane-bound proteins[15] or by a osmotically induced pearling instability[16].

There has been extensive research for protein mediated fission. The dynamin superfamily[8,18–20] or the ESCRT machinery[5,21,22] are two different sets of proteins that mediate in budding and fission. For example, the dynamin Drp1 is considered a major component in mitochondrial division; other dynamins are considered to either help or be necessary for the fission process. Previous numerical works on budding or fission at mesoscopic scales are based on the evolution of the membrane up to the instant prior to fission[23,24].

We have developed a three-dimensional model to study the dynamical evolution of a membrane, including not only the mean curvature energy term but also the Gaussian energy term. This is done by a phase-field methodology, which has been used to study a variety of systems based on the Helfrich theory for cellular membranes[25–34]. Numerical integration results show that without the inclusion of the Gaussian curvature the system exhibits a pearling instability, which has been already observed in many simulations[26,35,36] and experiments[37,38]. Pearling happens in membranes due to the spontaneous curvature, and the Gaussian curvature may lead to the fission of the pearls. Our phase field model explores the fission events where the Gaussian

curvature is relevant, and the results compare extremely well with the ones observed in experiments.

Methods

The model.—Phase-field approaches are suitable to model the dynamics of membranes that change their shape under certain conditions[25–33]. As the Gaussian curvature is an intrinsic property of the surfaces, no matter their dimensions or the metric relations that can be exerted within them[39], it certainly has an influence on the way membranes can change their shape. However, Gaussian curvature has not been considered in phase field models because its contribution to the energy is a topological invariant. Nonetheless, it has to be included in the study of membrane dynamics because the whole curvature energy depends on it and not only on the usual bending rigidity modulus due to the mean curvature. Minimization of the entire curvature energy allows to describe, not only the shape changes that membranes must acquire, but some processes that involve a change of genus, such as fission and fusion.

Starting off from the expression for the bending energy due the mean curvature H and the Gaussian curvature K we have

$$\mathscr{F} = \frac{\bar{\kappa}}{2}\int_\Gamma (2H - c_0)^2 ds + \bar{\kappa}' \int_\Gamma K ds, \tag{1}$$

where $\bar{\kappa}$ and $\bar{\kappa}'$ are the bending modulus and Gaussian modulus, c_0 is the spontaneous curvature and the integral is calculated over the whole membrane surface Γ. In here we include the influence of the Gaussian curvature K in the dynamics of the system in order to model situations in which the genus of the membrane changes.

In terms of the principal curvatures of the surface, the free energy of Eq. (1) can be written as follows:

$$\mathscr{F} = \frac{\bar{\kappa}}{2}\int_\Gamma \left(\frac{1}{R_1} + \frac{1}{R_2} - c_0\right)^2 ds + \bar{\kappa}' \int_\Gamma \left(\frac{1}{R_1 R_2}\right) ds, \tag{2}$$

where R_i are the principal radii of curvature. Note that the mean curvature has dimensions of inverse length, and the Gaussian curvature has dimensions of inverse length squared.

A phase-field model of the Cahn-Hilliard type can be defined from Eq. (1), as in Ref.[25], in which the authors express the free energy $\mathscr{F}$ of the system as an expansion of powers of a smooth scalar field $\phi : \Omega \subset \mathbf{R^3} \longrightarrow \mathbf{R}$, that acts as an order parameter:

$$\mathscr{F} = \int_\Omega \mathscr{L}(\phi, \nabla\phi, \nabla^2\phi) dV. \tag{3}$$

Assuming that the system is isotropic and homogeneous, and given that the order parameter must have two stable phases, the energy density $\mathscr{L}$ can be written as $\mathscr{L} = (\Phi[\phi])^2$, where the functional is defined as $\Phi[\phi] = -\phi + \phi^3 - \varepsilon^2\nabla^2\phi$.

The parameter ε represents the width of the interface between the two phases. One of the stable phases, typically defined by $\phi = 1$, corresponds to the interior of the volume delimited by the membrane located at $\phi = 0$, whereas $\phi = -1$ represents the outer environment.

It can be demonstrated that Eq. (3) with $\mathscr{L} = (\Phi[\phi])^2$ is equivalent to the expression of the bending energy of the surface in terms of the mean curvature H[25]. This would model the first half of Eq. (1), only the Gaussian term remains to be portrayed in a phase field approach.

The Gaussian curvature term can be defined in terms of the curvature tensor $Q_{\alpha\beta}$ of the surface as

$$K = \sum_{\alpha,\beta}\left[\left(Q_{\alpha\alpha}Q_{\beta\beta} - Q_{\alpha\beta}^2\right)\frac{1-\delta_{\alpha\beta}}{2}\right], \tag{4}$$

which in turn can be defined in terms of the gradients of the order parameter ϕ as[40],

$$Q_{\alpha\beta} = \frac{\sqrt{2}\varepsilon}{1-\phi^2}\left[\partial_{\alpha\beta}\phi + \frac{2\phi}{1-\phi^2}\partial_\alpha\phi\partial_\beta\phi\right], \tag{5}$$

where $\partial_\alpha = \partial/\partial x_\alpha$, and $\partial_{\alpha\beta} = \partial^2/\partial x_\alpha \partial x_\beta$.

The free energy $F = \mathscr{F}_{\mathscr{SC}} + \mathscr{F}_{\mathscr{G}}$ of the system is then represented by the spontaneous curvature model

$$\mathscr{F}_{\mathscr{SC}} = \kappa \int_\Omega \left((\phi - \varepsilon C_0)(\phi^2 - 1) - \varepsilon^2 \nabla^2 \phi\right)^2 dV, \tag{6}$$

where $\kappa = 3\sqrt{2}\bar{\kappa}/16\varepsilon^3$, $C_0 = c_0/\sqrt{2}$, plus the energy density due to the Gaussian curvature,

$$\mathscr{F}_{\mathscr{G}} = \frac{\kappa'}{2\varepsilon^2} \int_\Omega \tilde{K} dV = \frac{\kappa'}{2\varepsilon^2} \int_\Omega K(1-\phi^2)^2 dV$$

$$= \frac{\kappa'}{2\varepsilon^2} \int_\Omega \sum_{\alpha<\beta} (1-\phi^2)^2 \left[Q_{\alpha\alpha} Q_{\beta\beta} - Q_{\alpha\beta}^2\right] dV, \tag{7}$$

where $\kappa' = 3\sqrt{2}\varepsilon\bar{\kappa}'/4$. Both terms determine the complete bending energy of the system. The time evolution of the phase-field is set according to the Cahn-Hilliard dynamics, since the volume is supposed to be locally conserved[25–30]. The variations of the free energy with respect to ϕ must then be subjected to diffusion, yielding a dynamic equation for the phase-field governed by[25],

$$\frac{\partial \phi}{\partial t} = \nabla^2 \left(\frac{\delta \mathscr{F}_{\mathscr{SC}}}{\delta \phi} + \frac{\delta \mathscr{F}_{\mathscr{G}}}{\delta \phi} \right). \tag{8}$$

We can express this last equation in terms of the order parameter and its spatial variations only (see Appendix). The final result, after some algebra, is,

$$\frac{\partial \phi}{\partial t} = \kappa \nabla^2 \left((3\phi^2 - 1 - 2\phi\varepsilon C_0)\mu - \varepsilon^2 \nabla^2 \mu + \sigma[\phi]\nabla^2 \phi\right) - \kappa' \nabla^2 \left(\frac{12\phi}{1-\phi^2} F_{K_1} + \frac{2(3\phi^2+1)}{(1-\phi^2)^2} F_{K_2} \right), \tag{9}$$

where $\mu = (\phi - \varepsilon C_0)(\phi^2 - 1) - \varepsilon^2 \nabla^2 \phi$. The terms F_{K_i} represent the Gaussian curvature effect and are, explicitly,

$$F_{K_1} = \partial_{\alpha\alpha}\phi \partial_{\beta\beta}\phi - (\partial_{\alpha\beta}\phi)^2,$$

and

$$F_{K_2} = \partial_{\alpha\alpha}\phi (\partial_\beta \phi)^2 + \partial_{\beta\beta}\phi (\partial_\alpha \phi)^2 - 2\partial_{\alpha\beta}\phi \partial_\alpha \phi \partial_\beta \phi.$$

The parameter $\sigma[\phi]$ is a Lagrange multiplier that depends on the field ϕ and assures area conservation[40]. One can determine $\sigma[\phi]$ by calculating the area $S \propto \int_\Omega |\nabla\phi|^2 dV$ and demanding that $dS/dt \approx 0$. Using that Eq. (8) guarantees the conservation of the field ϕ, one obtains

$$\sigma[\phi] = -\frac{\int_\Omega \nabla\phi \cdot \nabla[\nabla^2 (\frac{\delta \mathscr{F}_{\mathscr{SC}}}{\delta\phi} + \frac{\delta \mathscr{F}_{\mathscr{G}}}{\delta\phi})] dV}{\int_\Omega \nabla\phi \cdot \nabla[\nabla^2(\nabla^2\phi)] dV}. \tag{10}$$

Results

Numerical simulations.–In principle, by solving Eqs. (9–10), it is possible to model situations in which the topological genus of the membrane changes, as in vesicle formation. Thus, we performed three dimensional calculations using the same method of integration as in[25]. We used a finite-difference scheme for the spatial discretization and an Euler method for the temporal derivatives with the appropriate time step of $dt = 10^{-5}$, small enough to avoid artefacts[41], as the initial membrane we choose a cylindrical shape of radius R and length L with a spherical cap. Its base is in contact with the wall of the domain and we are using zero flux boundary conditions.

We start with the simplest phenomenon, the formation of two closed membranes from one, the Gaussian curvature controlling the fission of a single vesicle. The results are shown in Fig. 1 for the cases when (a) the Gaussian curvature term is not included in the free energy, and (b) solving the complete dynamical equation (9).

For the case when the Gaussian curvature is not considered ($\kappa' = 0$ in Fig. 1(a)) a single neck forms, but there is no fission of the membrane. These results are consistent with previous works in which the Gaussian curvature is ignored[26].

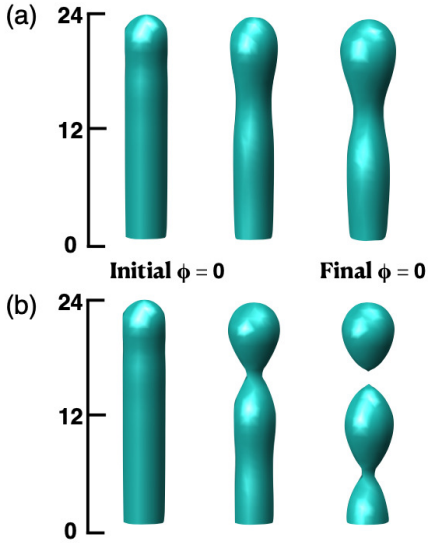

Figure 1. (a) Time evolution of the interface $\phi = 0$ without considering Gaussian curvature ($\kappa' = 0$). Snapshots of the membrane shape after two thousand, four million and ten millions of iterations (left to right). (b) Considering the Gaussian curvature contribution with $\kappa' = -10$. The snapshots are taken at the same time as in (a). The last snapshot depicts the exact moment when the vesicle breaks from the main membrane. The parameters used were: $R = 5$ and $L = 26$ in units of the domain grid and, $\kappa = 1$, $C_0 = -0.3$.

The addition of the Gaussian term in Eq. (9) makes the fission of the membrane energetically favorable and a vesicle is formed from the initial cylinder (Fig. 1(b)). We take $-\bar{\kappa}' \approx \bar{\kappa}$, as estimated in experiments and simulations alike[13,14]. The size of this system only allows the cylinder to make a single vesicle. The dimensions of the vesicles can be predicted by a dispersion relation calculation shown below.

For longer cylinders multiple fission events are possible. In Fig. 2, we show the results for a cylinder of length 45. We obtained a sequence of single fission events from the tip of the cylinder downwards. After ~ 270000 time iterations, the cylinder splits into five separate closed vesicles. Shape changes start simultaneously through the entire tube, but the speed of pearling and fission is not equal. The tip of the cylinder changes shape faster and splits first. In Fig. 2(a) we show the initial and final configurations of $\phi = 0$ for a longitudinal medial section of the tube.

The time evolution of the volume, the area, and the ratio λ = volume/area of the cylinder is shown in Fig. 2(b). The increments of the ratio λ (the onset bifurcations) are correlated with the beginning of vesicle formations.

Calculations on a longer cylinder are shown in Fig. 3. A pearling instability and an ordered fission is still observed. The onset of the pearling instability in Fig. 3 also appears on previous works[26], but here the pearls fission due to the Gaussian curvature contribution. We conclude that Gaussian curvature controls the formation of many small vesicles from one big elongated vesicle as seen in the experimental results[15,16].

All simulations were carried out having a reservoir of volume and area at the base of the cylinder. Therefore, global conservation of area and volume is not necessary. However, conservation of area and volume for individual vesicles should hold. As the vesicles fission from the main membrane, they lose contact with any reservoir of volume and area. Thus, from the moment they split, the vesicles must maintain their area and volume. In Fig. 2(b) it can be noticed that the area and volume vary slightly, although these values for the individual vesicles remain stable.

In order to analyse the stability of neck formation, it is possible to study the effects of small perturbations around the flat interface. These perturbations are taken as plane waves of the form $\phi = \phi_0 e^{i\mathbf{q}\cdot\mathbf{x}-\omega\mathbf{t}}$, near $\phi = 0$, with small amplitudes, $\phi_0 \ll 1$. Substituting these expressions into Eq. (9), and considering isotropic perturbations, one obtains the dispersion relation

$$\omega(q) = 3q^2\kappa\left[(1-2\varepsilon^2C_0^2)+12\delta\varepsilon C_0\right] - 9q^4\kappa\varepsilon^2\left[2(1+4\delta\varepsilon C_0)\right] - 9q^4\kappa\sigma + 27q^6\kappa\varepsilon^4. \tag{11}$$

Here, δ represents terms of order $\mathscr{O}(\phi^2)$. The detailed derivation of the dispersion relation is given in Appendix B. The main contribution to the instability comes from the first term in Eq. (11), in which the spontaneous curvature predominates. As the Gaussian curvature (due to κ') is not present in Eq. (11), it does not alter the region of unstable wavelengths. The Gaussian curvature acts by causing topological changes of the membrane right in the sites where the instability occurs.

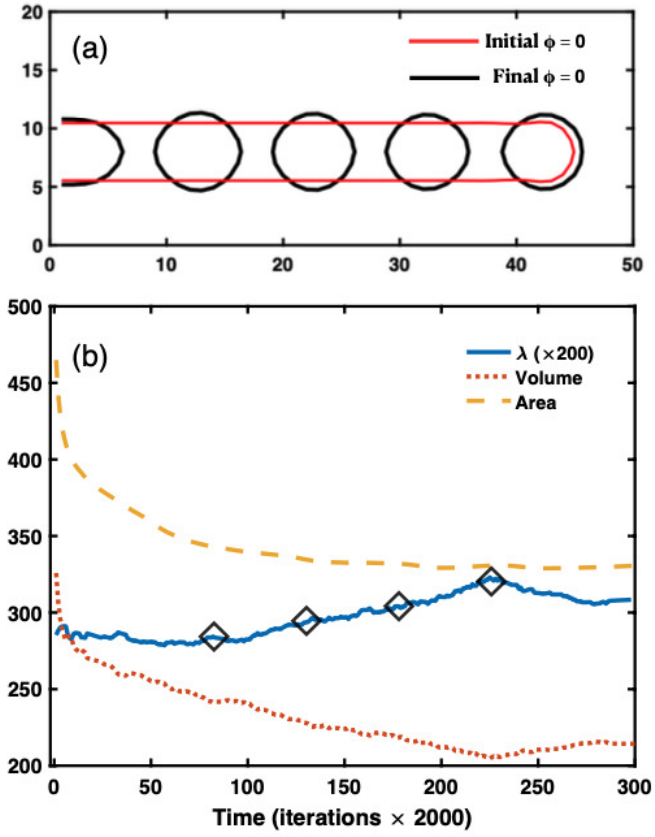

Figure 2. Time evolution of a longer membrane tube with Gaussian curvature. (a) Contour plots on the plane x,z of the initial (red) and final (black) $\phi = 0$ configuration. (b) Time variations of the volume (yellow dashed line), the area (red dotted line) and the ratio λ = volume/area (blue line). The open black diamonds over the λ curve represent the times where bifurcations occur. The parameters used were: $R = 6$ and $L = 45$, $\varepsilon = 1$, $\kappa' = -10$ and $C_0 = -0.5$.

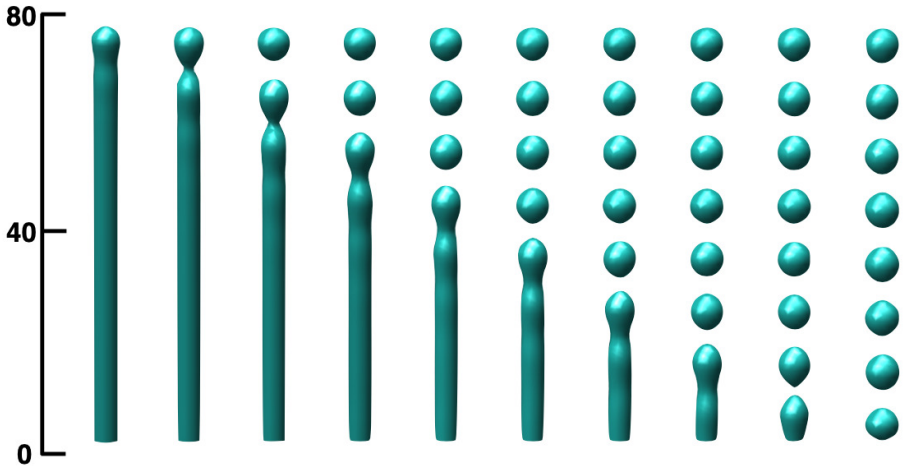

Figure 3. Snapshots of the evolution of the pearling instability in a long cylinder. Vesicles fission in sequence from the tip to the base. The parameters used were: $R = 6$, $L = 75$, $\varepsilon = 1$, $\kappa = 1$, $\kappa' = -10$ and $C_0 = -0.5$.

The periodicity of the instability is determined by a critical length, $l_c = \pi/q_c$, where $q_c > 0$ given by the point in which the unstable branch ceases to be positive $(\omega(q) = 0)$. This quantity represents a scale for the formation of the necks. The

dispersion relation for typical values of the parameters is depicted in Fig. 4. There, the corresponding values of the critical length in domain units are: $l_c \approx 7.6$ and $l_c \approx 10$ when $C_0 = -0.3$ and $C_0 = -0.5$, respectively. This is in agreement with the size (number) of vesicles formed in Figs. 1-3. For instance, in Fig. 3 eight vesicles can be formed in a tube of length $L = 75$ and a spontaneous curvature of $C_0 = -0.5$, as the critical length is $l_c \approx 10$ in domain units for this case. Similar results are observed for shorter cylinders and the corresponding values of C_0 in Figs. 1-2.

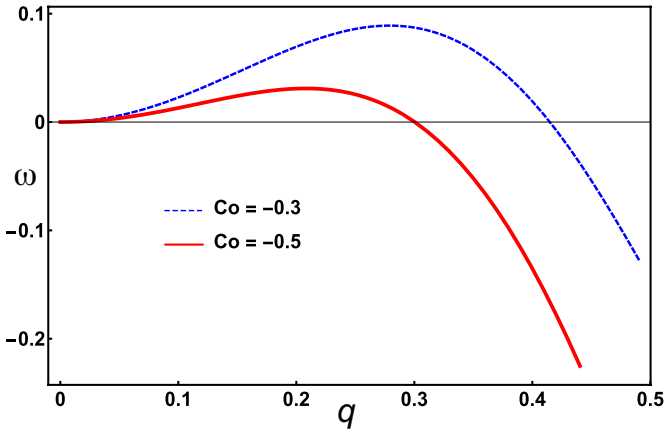

Figure 4. Dispersion relation with different values of spontaneous curvature. The parameter values are: $\kappa = 1$, $\varepsilon = 1$, $\delta = 0.001$ and $\sigma = 0.1$.

Finally, we explore the regime in which the Gaussian bending modulus κ' determines whether vesicle formation happens or not. The results in Fig. 5 show the equilibrium configurations for a single continuous membrane with tubular shape. For negative κ' the transition from a single vesicle to to many small vesicles, occurs along the line where $8\varepsilon^4\kappa + \kappa' = 0$ (dotted line in Fig. 5). When κ' is positive there is the formation of a multiple self-connected membrane, a continuous single membrane with multiple holes.

Discussion

We have studied the fission of membranes (vesicle formation) by extending the bending free energy model through the introduction of the Gaussian curvature. The Gaussian energy term provides the pearling instability the ability to fission from the initial membrane and maintain the stability of the system. With this model, multiple fission events can be obtained in a single computation.

The dynamics of vesicle formation was studied numerically and an ordered fission of the tube, from the tip to the base of the tube, was obtained. The number of formed vesicles depends on the dimensions of the tubular domain and the value of the spontaneous curvature. This number could be predicted using the dispersion relation obtained from a linear analysis of the model.

Topological changes were explored taking into account the two bending modules, giving us a membrane shape diagram. We corroborate the existence of multiple vesicles for negative κ' for the values $\kappa' < -8\varepsilon^4\kappa$. For Gaussian modulus $\kappa' > -8\varepsilon^4\kappa$ no topological transition occurs. For positive κ' the result is a multiple self-connected membrane.

To summarize, this model is able to reproduce experimental results where membrane tubes fission into several vesicles, such as[15,16]. The model can represent systems where special machinery is required for fission. Using the bending modulus and the Gaussian modulus we can obtain a membrane shape diagram, and we explored the membrane tube shape regimes. The specific mechanisms and molecular agents implicated in a biological context can be modeled using the Gaussian modulus.

References

1. Miserey-Lenkei, S. *et al.* Rab and actomyosin-dependent fission of transport vesicles at the golgi complex. *Nat. cell biology* **12**, 645–654 (2010).
2. Rothman, J. E. Mechanisms of intracellular protein transport. *Nature* **372**, 55–63 (1994).
3. Miesenböck, G., De Angelis, D. A. & Rothman, J. E. Visualizing secretion and synaptic transmission with ph-sensitive green fluorescent proteins. *Nature* **394**, 192–195 (1998).

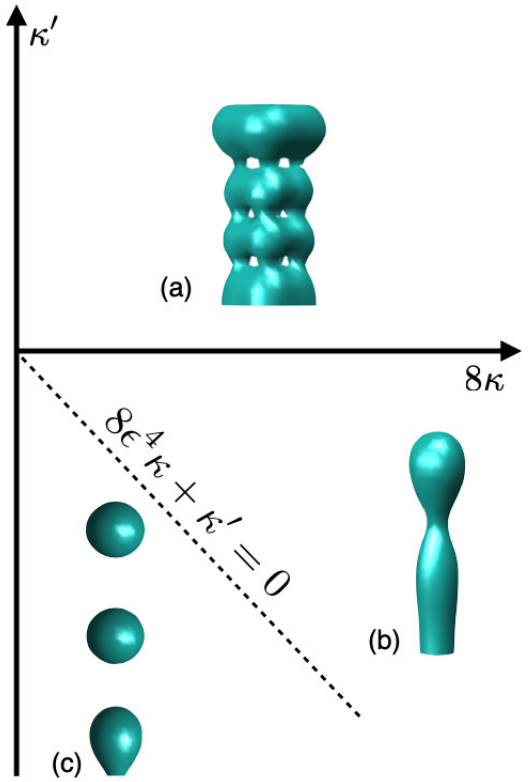

Figure 5. Membrane shape diagram for the (κ, κ') landscape with $\varepsilon = 1$. (a) Multiple self-connected membrane with positive κ', (b) neck formation without fission for $\kappa' > -8\kappa$, and (c) vesicle formation with a magnitude of $\kappa' < -8\kappa$.

4. Parkar, N. S. *et al.* Vesicle formation and endocytosis: function, machinery, mechanisms, and modeling. *Antioxidants & redox signaling* **11**, 1301–1312 (2009).

5. Dharmavaram, S., She, S. B., Lázaro, G., Hagan, M. F. & Bruinsma, R. Gaussian curvature and the budding kinetics of enveloped viruses. *PLoS computational biology* **15**, e1006602 (2019).

6. Eckert, D. M. & Kim, P. S. Mechanisms of viral membrane fusion and its inhibition. *Annu. review biochemistry* **70**, 777–810 (2001).

7. Cherry, J., Demmler-Harrison, G. J., Kaplan, S. L., Steinbach, W. J. & Hotez, P. J. *Feigin and Cherry's Textbook of Pediatric Infectious Diseases E-Book* (Elsevier Health Sciences, 2013).

8. Bassereau, P. *et al.* The 2018 biomembrane curvature and remodeling roadmap. *J. physics D: Appl. physics* **51**, 343001 (2018).

9. Campelo, F. & Malhotra, V. Membrane fission: the biogenesis of transport carriers. *Annu. review biochemistry* **81**, 407–427 (2012).

10. Helfrich, W. & Harbich, W. *Equilibrium Configurations of Fluid Membranes. In: Physics of Amphiphilic Layers* (Springer-Verlag, Berlin, 1987).

11. Do Carmo, M. P. *Differential geometry of curves and surfaces: revised and updated second edition* (Courier Dover Publications, 2016).

12. Fonda, P., Al-Izzi, S. C., Giomi, L. & Turner, M. S. Measuring gaussian rigidity using curved substrates. *Phys. Rev. Lett.* **125**, 188002, DOI: 10.1103/PhysRevLett.125.188002 (2020).

13. Siegel, D. P. & Kozlov, M. The gaussian curvature elastic modulus of n-monomethylated dioleoylphosphatidylethanolamine: relevance to membrane fusion and lipid phase behavior. *Biophys. journal* **87**, 366–374 (2004).

14. Hu, M., Briguglio, J. J. & Deserno, M. Determining the gaussian curvature modulus of lipid membranes in simulations. *Biophys. journal* **102**, 1403–1410 (2012).

15. Snead, W. T. *et al.* Membrane fission by protein crowding. *Proc. Natl. Acad. Sci.* **114**, E3258–E3267 (2017).

16. Sanborn, J., Oglĕcka, K., Kraut, R. S. & Parikh, A. N. Transient pearling and vesiculation of membrane tubes under osmotic gradients. *Faraday discussions* **161**, 167–176 (2013).

17. Farge, E. & Devaux, P. F. Shape changes of giant liposomes induced by an asymmetric transmembrane distribution of phospholipids. *Biophys. journal* **61**, 347–357 (1992).

18. Schmid, S. L. & Frolov, V. A. Dynamin: functional design of a membrane fission catalyst. *Annu. review cell developmental biology* **27**, 79–105 (2011).

19. Hinshaw, J. E. & Schmid, S. L. Dynamin self-assembles into rings suggesting a mechanism for coated vesicle budding. *Nature* **374**, 190–192 (1995).

20. Sweitzer, S. M. & Hinshaw, J. E. Dynamin undergoes a gtp-dependent conformational change causing vesiculation. *Cell* **93**, 1021–1029 (1998).

21. Bleck, M. *et al.* Temporal and spatial organization of escrt protein recruitment during hiv-1 budding. *Proc. Natl. Acad. Sci.* **111**, 12211–12216 (2014).

22. Van Engelenburg, S. B. *et al.* Distribution of escrt machinery at hiv assembly sites reveals virus scaffolding of escrt subunits. *Science* **343**, 653–656 (2014).

23. Kumar, P. S., Gompper, G. & Lipowsky, R. Budding dynamics of multicomponent membranes. *Phys. review letters* **86**, 3911 (2001).

24. Vasan, R., Rudraraju, S., Akamatsu, M., Garikipati, K. & Rangamani, P. A mechanical model reveals that non-axisymmetric buckling lowers the energy barrier associated with membrane neck constriction. *Soft Matter* **16**, 784–797 (2020).

25. Campelo, F. & Hernandez-Machado, A. Dynamic model and stationary shapes of fluid vesicles. *The Eur. Phys. J. E* **20**, 37–45 (2006).

26. Campelo, F. & Hernández-Machado, A. Model for curvature-driven pearling instability in membranes. *Phys. review letters* **99**, 088101 (2007).

27. Campelo, F. & Hernández-Machado, A. Polymer-induced tubulation in lipid vesicles. *Phys. review letters* **100**, 158103 (2008).

28. Campelo, F., Cruz, A., Pérez-Gil, J., Vázquez, L. & Hernández-Machado, A. Phase-field model for the morphology of monolayer lipid domains. *The Eur. Phys. J. E* **35**, 49 (2012).

29. Lázaro, G. R., Pagonabarraga, I. & Hernández-Machado, A. Phase-field theories for mathematical modeling of biological membranes. *Chem. physics lipids* **185**, 46–60 (2015).

30. Rueda-Contreras, M. D., Romero-Arias, J. R., Aragon, J. L. & Barrio, R. A. Curvature-driven spatial patterns in growing 3d domains: A mechanochemical model for phyllotaxis. *PloS one* **13**, e0201746 (2018).

31. Lázaro, G. R., Hernández-Machado, A. & Pagonabarraga, I. Rheology of red blood cells under flow in highly confined microchannels: I. effect of elasticity. *Soft Matter* **10**, 7195–7206 (2014).

32. Du, Q., Liu, C. & Wang, X. A phase field approach in the numerical study of the elastic bending energy for vesicle membranes. *J. Comput. Phys.* **198**, 450–468 (2004).

33. Barrio, R., Alarcon, T. & Hernandez-Machado, A. The dynamics of shapes of vesicle membranes with time dependent spontaneous curvature. *PloS one* **15**, e0227562 (2020).

34. Helfrich, W. Elastic properties of lipid bilayers: theory and possible experiments. *Zeitschrift für Naturforschung C* **28**, 693–703 (1973).

35. Su, Y.-C. & Chen, J. Z. A model of vesicle tubulation and pearling induced by adsorbing particles. *Soft Matter* **11**, 4054–4060 (2015).

36. Raote, I. *et al.* A physical mechanism of tango1-mediated bulky cargo export. *eLife* **9**, e59426 (2020).

37. Tsafrir, I. *et al.* Pearling instabilities of membrane tubes with anchored polymers. *Phys. review letters* **86**, 1138 (2001).

38. Yu, Y. & Granick, S. Pearling of lipid vesicles induced by nanoparticles. *J. Am. Chem. Soc.* **131**, 14158–14159 (2009).

39. Spivak, M. *A Comprehensive Introduction to Differential Geometry. Vol. 2* (Publish or Perish, INC., Houston, Texas, 1999).

40. Campelo, F. *Shapes in cells. Dynamic instabilities, morphology, and curvature in biological membranes.* (Universitat de Barcelona, Spain, 2008).

41. Strikwerda, J. *Finite difference schemes and partial differential equations* (Wadsworth & Brooks, Pacific Grove, 1989).

Acknowledgements

A.F.G. acknowledges financial support from MINECO (Spain) project FIS2016-78883-C2-1-P. Likewise, J.R.R.A. thanks to Ana Pérez-Arteaga and Ramiro Chávez-Tovar for their technical support, and the IIMAS Department of Mathematics and Mechanics for allowing him to join its group of researchers. A.H.M. acknowledges financial support from Ministerio de Ciencia e Innovación (Spain) project PID2019-1060636B-100. R.A.B. was financially supported by Conacyt through project 283279.

Author contributions statement

A.H.M. and R.A.B. devised the project and the main conceptual ideas. M.D.R.C., J.R.R.A, A.H.M., and R.A.B. developed the theory. M.D.R.C., A.F.G., J.R.R.A. and R.A.B. performed the numerical simulations. All authors discussed the results and contributed to the final manuscript.

Competing interests

The authors declare no competing interests.

Additional information

Correspondence and requests for materials should be addressed to J.R.R.A.

Appendix

Appendix A: Calculation of the complete dynamic equation for ϕ

Variations of $\mathscr{F}_{\mathscr{SC}}$ in Eq. (8) are explicitly,

$$\frac{\delta \mathscr{F}_{\mathscr{SC}}}{\delta \phi} = (3\phi^2 - 1 - 2\phi\varepsilon C_0)\mu - \varepsilon\nabla^2\mu + \sigma[\phi]\nabla^2\phi, \tag{12}$$

where

$$\mu[\phi] = (\phi - \varepsilon C_0)(\phi^2 - 1) - \varepsilon^2\nabla^2\phi, \tag{13}$$

is the chemical potential and $\sigma[\phi]$ is the surface tension coefficient, which is implemented as a Lagrange multiplier that ensures local area conservation.

It is necessary to express equation (1) in terms of ϕ so we might be able to establish the variations of the energy due to the Gaussian curvature similar to Eq. (12). These variations must also be subject to diffusion so we can obtain the dynamic equation that dictates the evolution of the surface. Variations of the free energy due to the Gaussian curvature can be written as

$$\frac{\delta \mathscr{F}_{\mathscr{G}}}{\delta \phi} = \frac{\partial \tilde{K}}{\partial \phi} - \partial_\gamma \cdot \frac{\partial \tilde{K}}{\partial(\partial_\gamma \phi)} + \partial_\gamma \partial_\gamma \cdot \frac{\partial \tilde{K}}{\partial(\partial_\gamma \partial_\gamma \phi)}. \tag{14}$$

We write this last equation in terms of the curvature tensor $Q_{\alpha\beta}$, that is, in terms of the gradients of ϕ, and then calculate each of the terms of Eq. (14) separately.

First, variations of $\tilde{K}$ with respect to ϕ can be written as:

$$\frac{\partial \tilde{K}}{\partial \phi} = \frac{2\sqrt{2}\varepsilon(\phi^2+1)}{1-\phi^2}\left[(\partial_\alpha\phi)^2 Q_{\beta\beta} + (\partial_\beta\phi)^2 Q_{\alpha\alpha}\right] - \frac{2\sqrt{2}\varepsilon(\phi^2+1)}{1-\phi^2}\left[2\partial_\alpha\phi\partial_\beta\phi Q_{\alpha\beta}\right]. \tag{15}$$

The second term of Eq. (14) is

$$\partial_\gamma \cdot \frac{\partial \tilde{K}}{\partial(\partial_\gamma\phi)} = \frac{4\sqrt{2}\varepsilon(1-3\phi^2)}{1-\phi^2}\left[(\partial_\alpha\phi)^2 Q_{\beta\beta} + (\partial_\beta\phi)^2 Q_{\alpha\alpha}\right] - \frac{4\sqrt{2}\varepsilon(1-3\phi^2)}{1-\phi^2}\left[2\partial_\alpha\phi\partial_\beta\phi Q_{\alpha\beta}\right] + 8\phi(1-\phi^2)\left(Q_{\alpha\alpha}Q_{\beta\beta} - Q_{\alpha\beta}^2\right), \tag{16}$$

and the third term is:

$$\partial_\gamma\partial_\gamma\cdot\frac{\partial\tilde{K}}{\partial(\partial_\gamma\partial_\gamma\phi)}=-4\phi(1-\phi^2)\left[Q_{\alpha\alpha}Q_{\beta\beta}-Q_{\alpha\beta}^2\right]+4\sqrt{2}\varepsilon\phi^2\left[(\partial_\alpha\phi)^2Q_{\beta\beta}+(\partial_\beta\phi)^2Q_{\alpha\alpha}\right]+4\sqrt{2}\varepsilon\phi^2(-2\partial_\alpha\phi\partial_\beta\phi Q_{\alpha\beta}). \tag{17}$$

By adding up equations (15), (16) and (17), and grouping similar terms we have:

$$\begin{aligned}\frac{\delta\mathscr{F}_\mathscr{G}}{\delta\phi}=&-12\phi(1-\phi^2)\left[Q_{\alpha\alpha}Q_{\beta\beta}-Q_{\alpha\beta}^2\right]+\frac{2\sqrt{2}\varepsilon(9\phi^2-1)}{1-\phi^2}\left[(\partial_\alpha\phi)^2Q_{\beta\beta}+(\partial_\beta\phi)^2Q_{\alpha\alpha}\right]\\&-\frac{2\sqrt{2}\varepsilon(9\phi^2-1)}{1-\phi^2}\left[2\partial_\alpha\phi\partial_\beta\phi Q_{\alpha\beta}\right].\end{aligned} \tag{18}$$

It is possible to express the variations of the free energy due to the Gaussian curvature in terms of $\tilde{K}$ itself:

$$\frac{\delta\mathscr{F}_\mathscr{G}}{\delta\phi}=\frac{(9\phi^2-1)}{\phi^2+1}\frac{\partial\tilde{K}}{\partial\phi}-\frac{12\phi}{1-\phi^2}\tilde{K}. \tag{19}$$

It is notable that the second term has a singularity when $\phi=\pm1$ (that is, in the bulk) and it also approaches to zero near the interface $\phi=0$. Thus, the main contribution to the curvature energy of the surface comes from the first term of Eq. (19), which depends on the variation of the Gaussian curvature with respect to the order parameter ϕ.

It is more appropriate to write the dynamical equations in terms of ϕ. Thus, equation (19) is equivalent to

$$\frac{\delta\mathscr{F}_\mathscr{G}}{\delta\phi}=2\varepsilon^2\frac{-12\phi}{1-\phi^2}\left[\partial_{\alpha\alpha}\phi\partial_{\beta\beta}\phi-(\partial_{\alpha\beta}\phi)^2\right]-2\varepsilon^2\frac{2(3\phi^2+1)}{(1-\phi^2)^2}\left[\partial_{\alpha\alpha}\phi(\partial_\beta\phi)^2+\partial_{\beta\beta}\phi(\partial_\alpha\phi)^2\right]+2\varepsilon^2\frac{4(3\phi^2+1)}{(1-\phi^2)^2}\left[\partial_{\alpha\beta}\phi\partial_\alpha\phi\partial_\beta\phi\right]. \tag{20}$$

The dynamic equation that dictates the evolution of the surface is

$$\begin{aligned}\frac{\partial\phi}{\partial t}=&\kappa\nabla^2\left((3\phi^2-1-2\phi\varepsilon C_0)\mu-\varepsilon\nabla^2\mu+\sigma[\phi]\nabla^2\phi\right)-\kappa'\nabla^2\left(\frac{12\phi}{1-\phi^2}\left[\partial_{\alpha\alpha}\phi\partial_{\beta\beta}\phi-(\partial_{\alpha\beta}\phi)^2\right]\right)\\&-\kappa'\nabla^2\left(\frac{2(3\phi^2+1)}{(1-\phi^2)^2}\left[\partial_{\alpha\alpha}\phi(\partial_\beta\phi)^2+\partial_{\beta\beta}\phi(\partial_\alpha\phi)^2\right]\right)+\kappa'\nabla^2\left(\frac{4(3\phi^2+1)}{(1-\phi^2)^2}\left[\partial_{\alpha\beta}\phi\partial_\alpha\phi\partial_\beta\phi\right]\right),\end{aligned} \tag{21}$$

which is defined only in terms of ϕ and its gradients and $\kappa'=3\sqrt{2}\varepsilon\bar{\kappa}'/4$.

Appendix B: Dispersion relation

In order to analyse the stability of the membrane, one can study the effect of small perturbations of the flat interface. In particular, one considers that perturbations take the form of plane waves: $\phi=\phi_0e^{i\mathbf{q}\cdot\mathbf{x}-\omega\mathbf{t}}$, where $\mathbf{q}=q_\alpha$ and $\mathbf{x}=x_\alpha$ are the wave vector and Cartesian coordinates ($\alpha=1,2,3$), around the membrane $\phi=0$. We assume that the amplitude $\phi_0\ll1$ is small.

Taking into account Eq. (9) of the main text and substituting the approximation in each term, one obtains

$$\begin{aligned}\nabla^2\left((3\phi^2-1-2\phi\varepsilon C_0)\mu\right)=&-q_\alpha^2\phi\left[(3\phi^2-1-2\phi\varepsilon C_0)^2+(6\phi-2\varepsilon C_0)(\phi-\varepsilon C_0)(\phi^2-1)\right]-q_\alpha^4\varepsilon^2\phi\left[(3\phi^2-1-2\phi\varepsilon C_0)\right.\\&\left.+\phi(6\phi-2\varepsilon C_0)\right],\end{aligned} \tag{22}$$

since

$$\nabla^2\mu=-q_\alpha^2\phi(3\phi^2-1-2\phi\varepsilon C_0)-q_\alpha^4\varepsilon^2\phi. \tag{23}$$

The next term on the right hand side of Eq. (9) is,

$$\nabla(-\varepsilon^2\nabla\mu) = -q_\alpha^4\varepsilon^2\phi\left[(3\phi^2-1-2\phi\varepsilon C_0)+\phi(6\phi-2\varepsilon C_0)\right]-q_\alpha^6\varepsilon^4\phi. \tag{24}$$

On the other hand, one obtains,

$$F_{K_1} = F_{K_2} = 0. \tag{25}$$

The last equality is to be expected since in the plane wave approximation the functional associated with the Gaussian curvature is

$$\tilde{K} = \sum_{\alpha<\beta}(1-\phi^2)^2\left[Q_{\alpha\alpha}Q_{\beta\beta}-Q_{\alpha\beta}^2\right] = 0. \tag{26}$$

Now, if one substitutes equations B1-B4 in Eq. (9), one obtains

$$\begin{aligned}\omega(q)\phi = {} & q_\alpha^2\kappa\phi\left[(6\phi-2\varepsilon C_0)(\phi-\varepsilon C_0)(\phi^2-1)+(3\phi^2-1-2\phi\varepsilon C_0)^2\right]+q_\alpha^4\kappa\varepsilon^2\phi\left[2\phi(6\phi-2\varepsilon C_0)+2(3\phi^2-1-2\phi\varepsilon C_0)\right]\\ & -q_\alpha^4\kappa\sigma\phi+q_\alpha^6\kappa\varepsilon^4\phi.\end{aligned} \tag{27}$$

Assuming an isotropic perturbation $q_\alpha = q$ with small wave number, and using $\phi := \delta$ for the terms of the order $\mathscr{O}(\phi^2)$, one finally obtains the dispersion relation

$$\omega(q) = 3q^2\kappa\left[(1-2\varepsilon^2C_0^2)+12\delta\varepsilon C_0\right]-9q^4\kappa\varepsilon^2\left[2(1+4\delta\varepsilon C_0)\right]-9q^4\kappa\sigma+27q^6\kappa\varepsilon^4. \tag{28}$$

From this result, one observes that the spontaneous curvature is responsible for the onset of the instability and that the mean and Gaussian curvature do not affect the region of the unstable wavelengths.

Figures

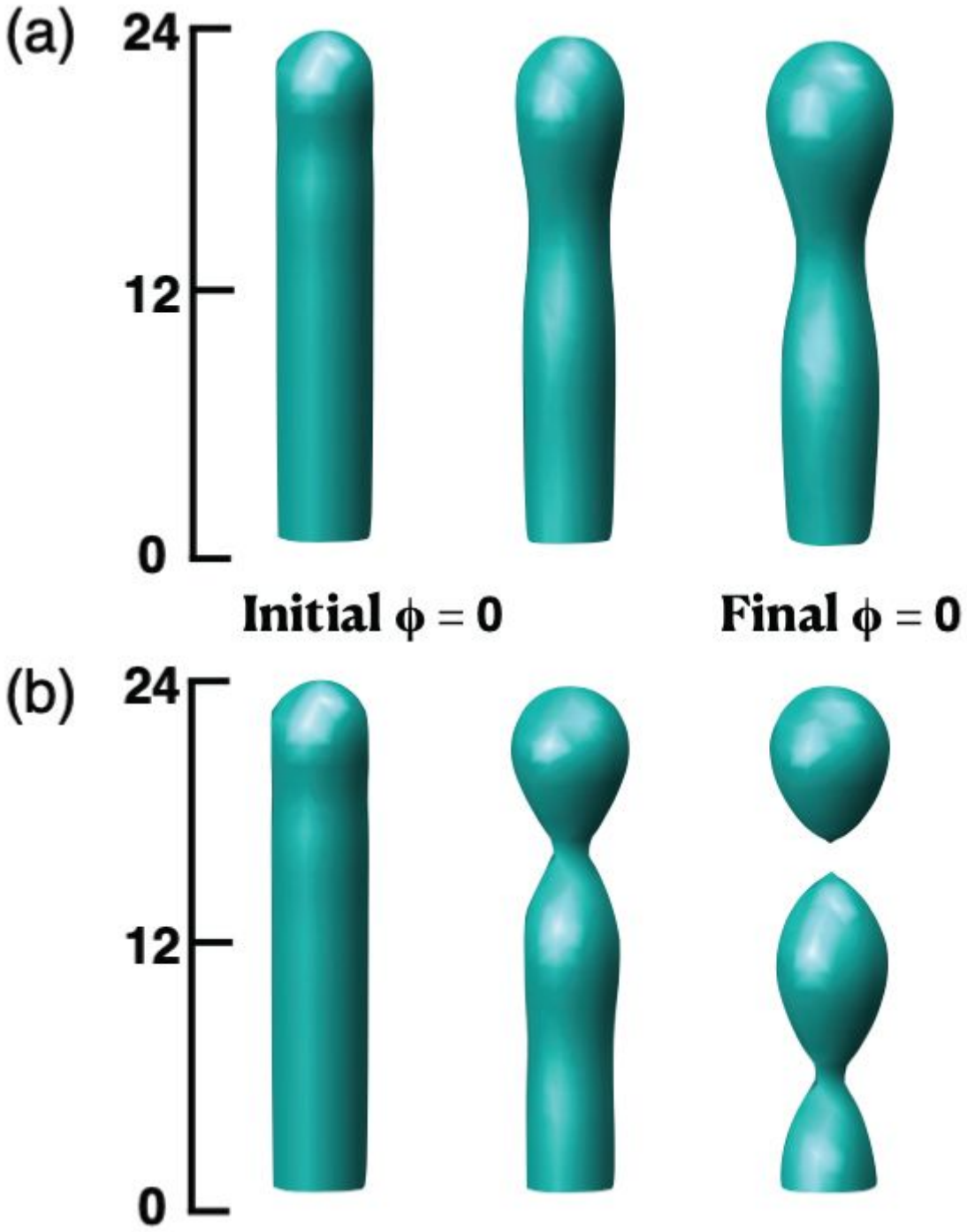

Figure 1

"Please see the Manuscript PDF file for the complete figure caption".

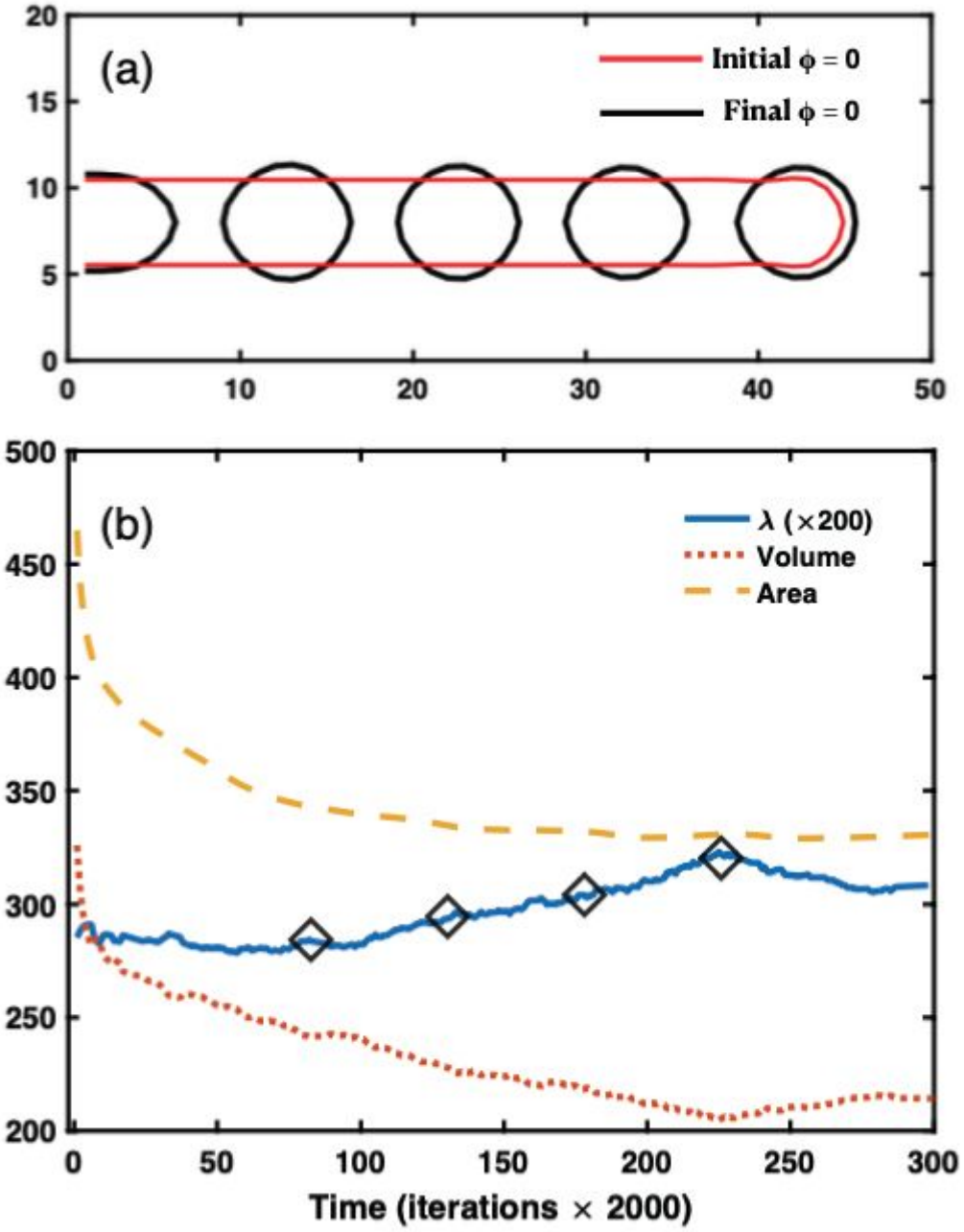

Figure 2

"Please see the Manuscript PDF file for the complete figure caption".

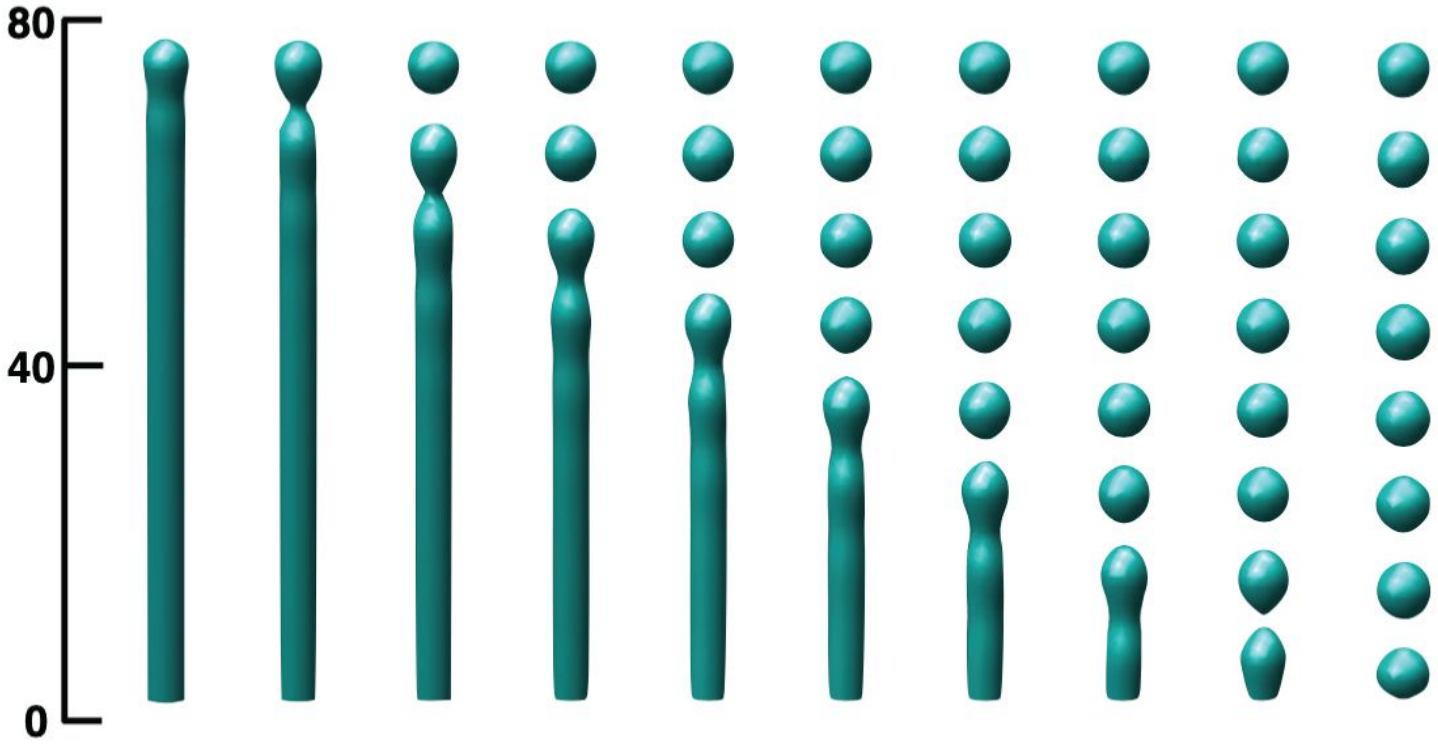

Figure 3

Snapshots of the evolution of the pearling instability in a long cylinder. Vesicles fission in sequence from the tip to the base. The parameters used were: R = 6, L = 75, e = 1, k = 1, k0 = -10 and C0 = -0:5.

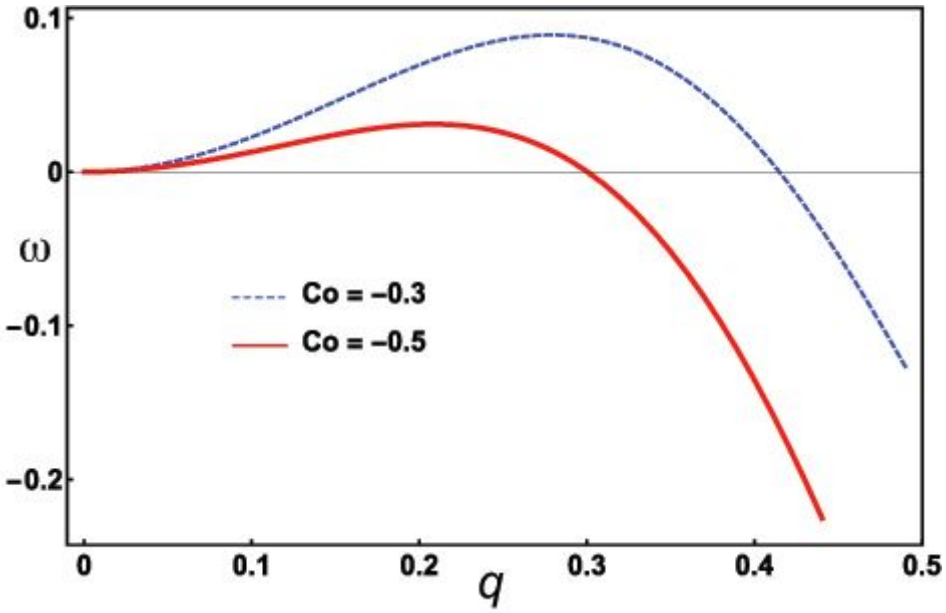

Figure 4

Dispersion relation with different values of spontaneous curvature. The parameter values are: k = 1, ε = 1, δ = 0:001 and σ = 0:1.

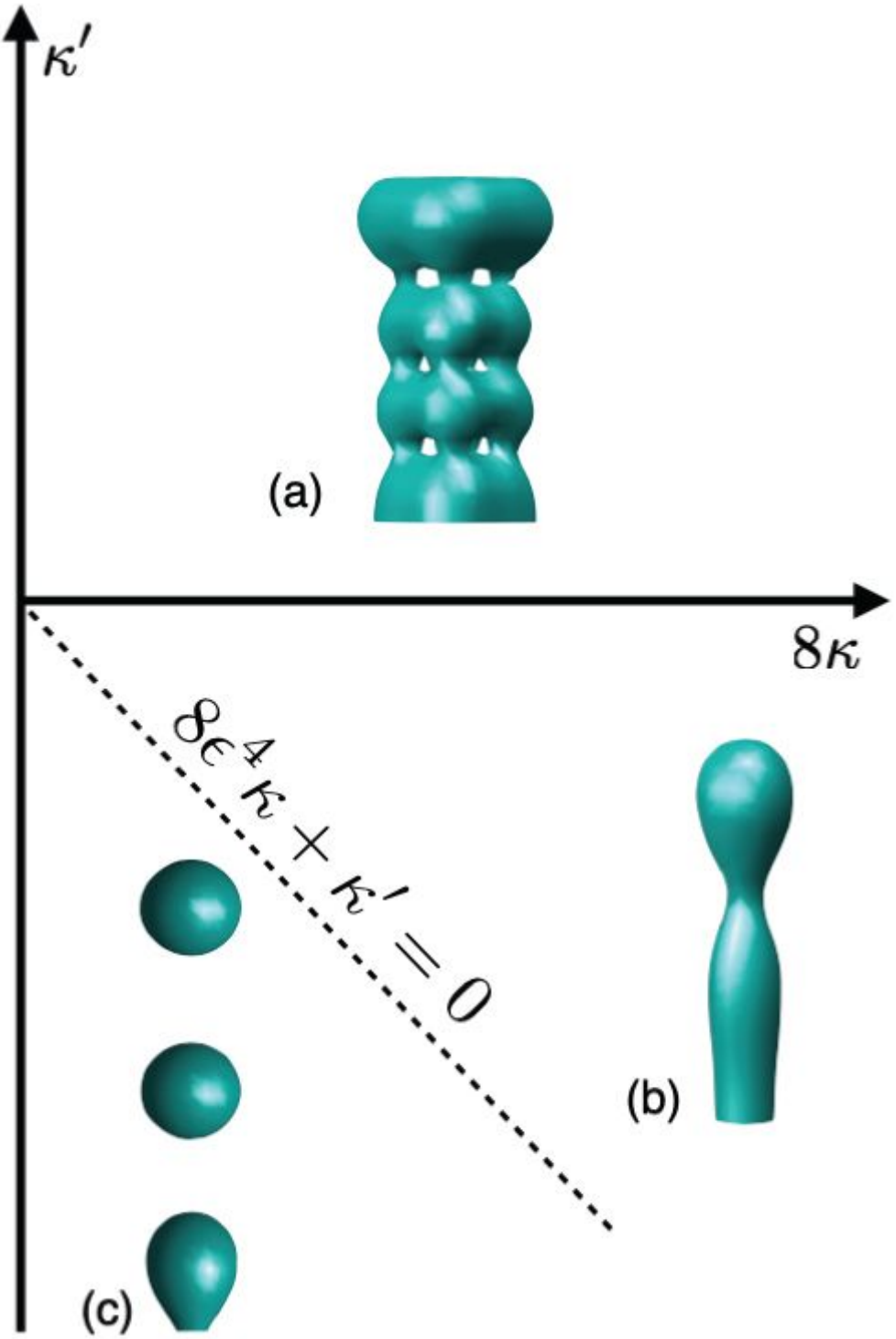

Figure 5

"Please see the Manuscript PDF file for the complete figure caption".